

Performance of HgCdTe Infrared Detectors with 5-10 μm Cutoff Wavelengths at 20-50K Operating Temperatures

Robert Bailey, Jose Arias, Will McLevige, John Pasko, Annie Chen,
Craig Cabelli, John Blackwell, Lester Kozlowski, and Kadri Vural

Rockwell Science Center, 1049 Camino dos Rios, Thousand Oaks, CA 91360

Sheldon Weng, Jian Wu, William Forrest, and Judith Pipher

University of Rochester, Dept. of Physics and Astronomy, Rochester, NY 14627

This work was partially supported by NASA contracts NAGW-2392 and NAG5-6267 and by NSF contract AST9630625

NGST Requires Extensions of HgCdTe FPA Technology Developed for Many Very Different Applications

RBB, NGST, 6/3/98, 2

Applications

strategic defense
seekers
imaging cameras
remote sensing
spectroscopy
astronomy

Requirements

wavelength
operating temperature
background flux
pixel format, pitch
noise
integration time
frame rate

NGST Goals and Requirements

5-10 μm cutoff
temperature $\approx 30\text{K}$
0.1 - 1000 photons/sec
• low defect density
• low dark current
• low noise
• high QE
2048x2048
visible response

4 Key Hybrid FPA Technologies

Molecular Beam Epitaxy HgCdTe
double layer crystal growth

p-on-n double layer planar
heterojunction photovoltaic detector
array fabrication

CMOS readout integrated circuit
design and fabrication

balanced composite structure
hybrid assembly and packaging

For $\lambda_c \geq 5 \mu\text{m}$ HgCdTe Has Potential for Higher Operating Temperature than InSb or Si:As

RBB, NGST, 6/3/98, 3

	InSb	Si:As	Hg _{1-x} Cd _x Te		
Cutoff Wavelength (μm)	5.5	>20	2.5	5-10	5-10
Operating Temperature	20-30K	<10K	78K	20-50K	20-50K
Substrate	InSb	Silicon	Al ₂ O ₃	CdZnTe	silicon
Substrate Removal	yes	no	no	no	no
Pixel Yield	high	highest	high	lower	lowest
Readout Integrated Circuit	CMOS	Custom CMOS	CMOS	CMOS	CMOS
Readout/Detector Thermal Expansion Mismatch	Thinned InSb conforms	None	Thinned readout conforms	Thinned readout conforms	None

Rockwell is just beginning to produce and test FPAs with $\lambda_c \geq 5 \mu\text{m}$ optimized for low background astronomy. Much more data is needed for tradeoff analysis involving λ_c , temperature, dark current, QE, pixel yield, uniformity, etc.

Summary of Progress Toward NGST Goals

RBB, NGST, 6/3/98, 4

University of Rochester collaboration

- 1st program, begun in 1991, tested 5 μm cutoff HgCdTe detectors and arrays on both Al_2O_3 and CdZnTe substrates. Pixel yields were not competitive with InSb.
- Ongoing programs have goals of 10 μm cutoff wavelength, 30K operating temperature, and dark currents < zodiacal background current of ≈ 1000 e-/sec.
 - Many $\lambda_c = 10.6$ μm test detectors have $I_{\text{dark}} < 10^4$ e-/sec @ 30K. One had < 1000 e-/sec
 - Tunneling current model suggests potential 10x dark current reduction for modest detector base layer doping decrease
 - First 256x256 FPAs fabricated specifically for this application are being assembled this week.

Summary of Progress Toward NGST Goals

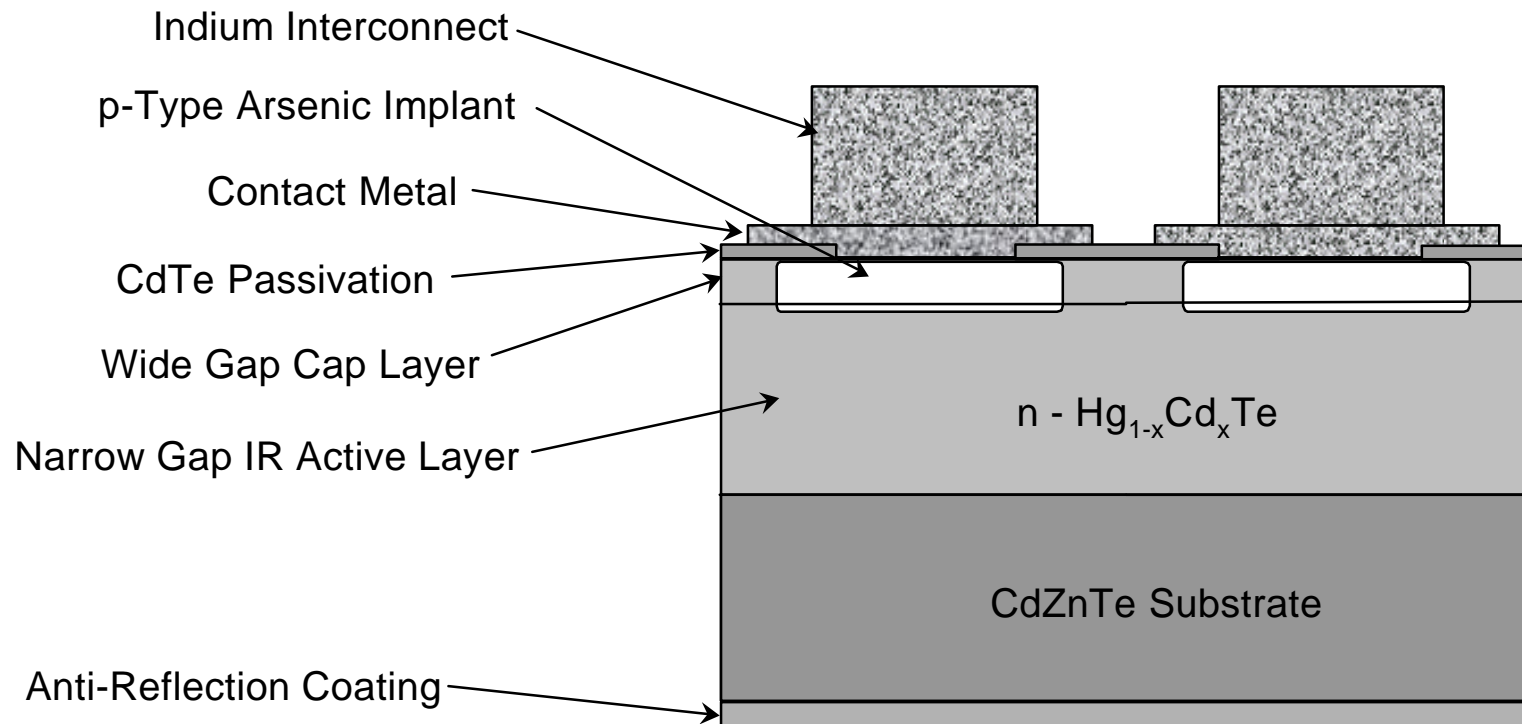
RBB, NGST, 6/3/98, 5

- 2048x2048 readout design includes multiple outputs to allow fast readout to handle higher photocurrents from 5 μm detectors
- For $\lambda_c = 5.2 \mu\text{m}$ and CdZnTe detector substrate, mean $I_{\text{dark}} = 0.39 \text{ e-/sec}$ @ 50K for 1 quadrant of PICNIC 256x256 FPA
- Large, reliable hybrid FPAs have been produced and tested to demonstrate the effectiveness of the balanced composite structure:
 - Silicon detector substrate:
 - 1024x1024 pixels, 18 μm pitch
 - $\lambda_c = 4.2 \mu\text{m}$, QE = 0.58, 99.65% pixel yield, 5.4% response nonuniformity
 - CdZnTe detector substrate
 - 640x480 pixels, 27 μm pitch
 - $\lambda_c = 5.0 \mu\text{m}$, QE = 0.81, 98.2% pixel yield, 4.8% response nonuniformity

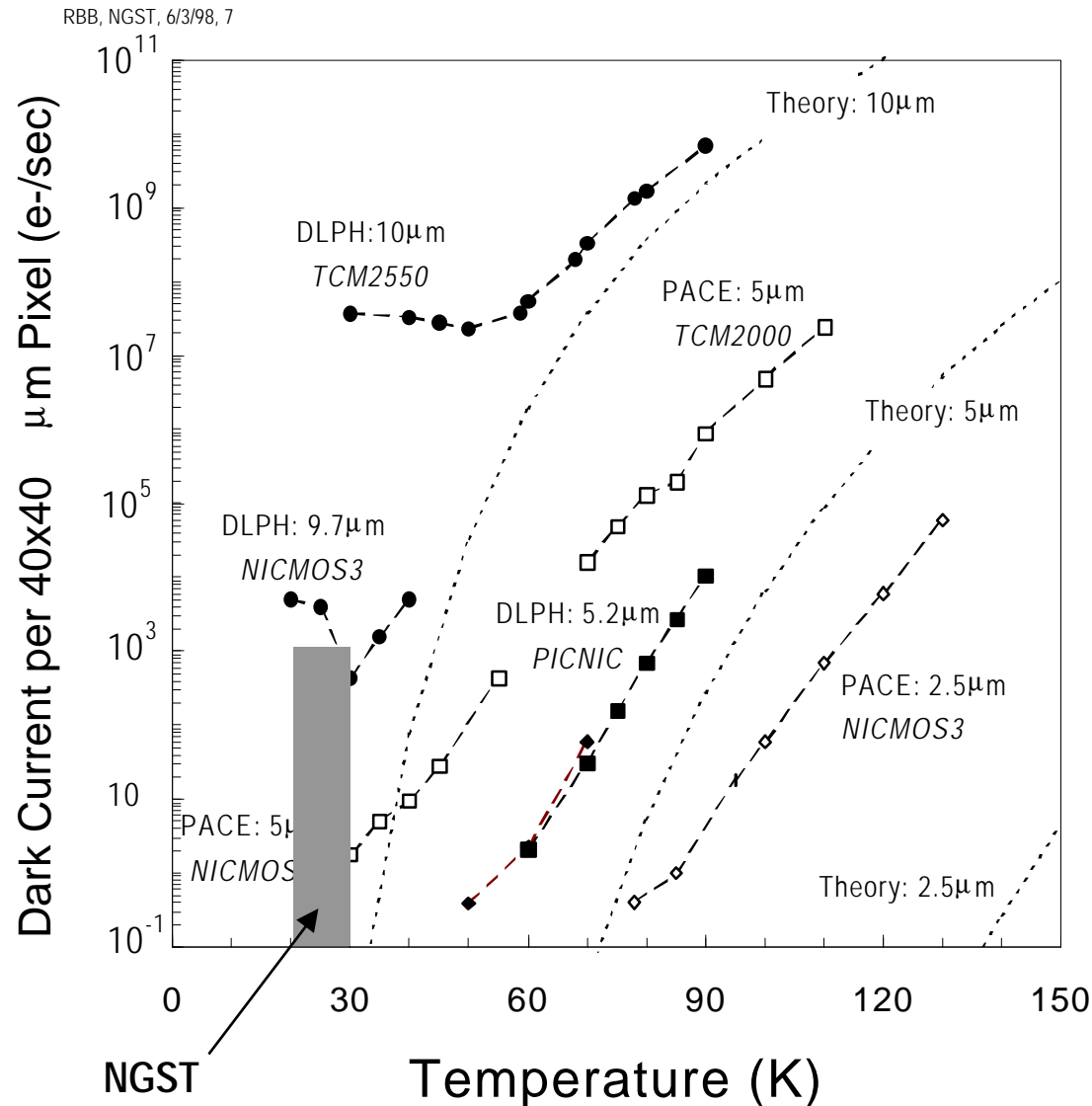
Molecular Beam Epitaxy Double Layer Planar Heterostructure (DLPH) Detectors

RBB, NGST, 6/3/98, 6

- Precise control over layer doping, thickness, and composition variable x
- Low temperature crystal growth
- Lattice matched substrate reduces HgCdTe crystal defect density
- Wide band gap cap layer is easier to passivate.



5.2 μm DLPH has 100x lower I_{dark} than 5 μm PACE



I_{dark} follows ideal diode T and λ_c dependence at high temperature with excess current from crystal defect and impurity states

5.2 μm median $I_{\text{dark}} = 0.39$
@50K and 0.5V bias on 128x128 quadrant of PICNIC FPA

Nonuniform tunneling and shunt currents with weak temperature dependence become significant at the lowest temperatures

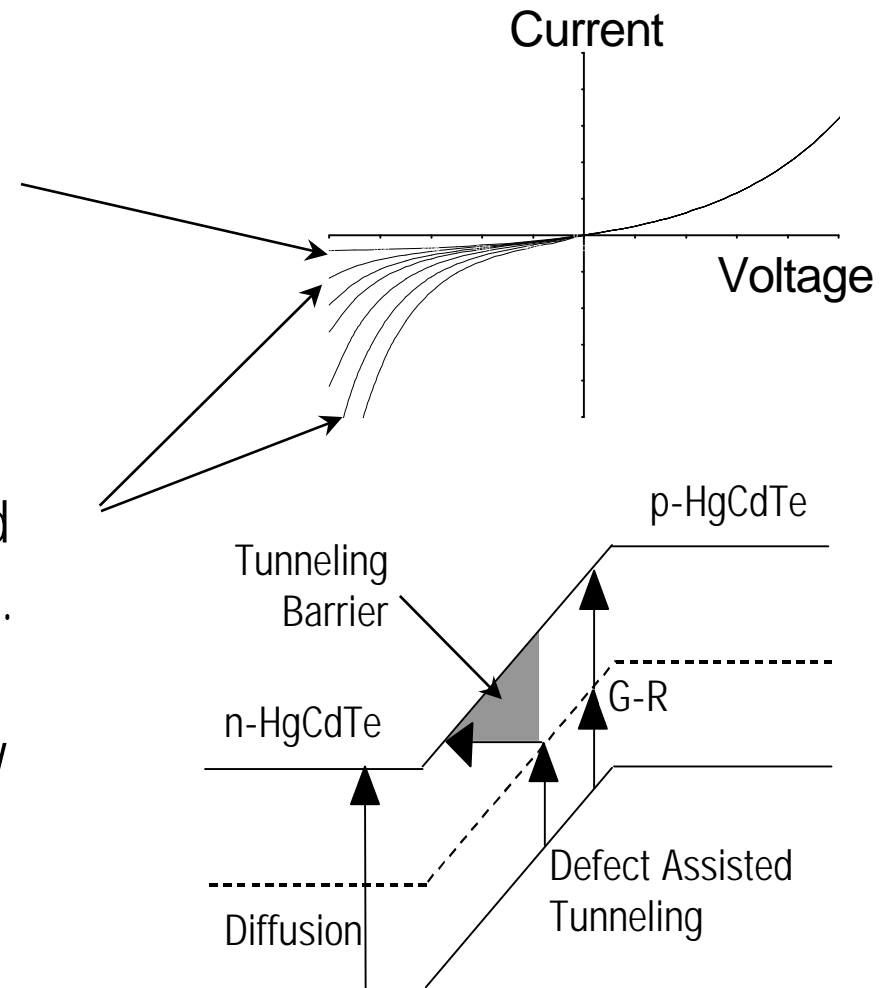
λ_c values in plot are @ 77K

Dark Current Sources in HgCdTe Photovoltaic Detectors

RBB, NGST, 6/3/98, 8

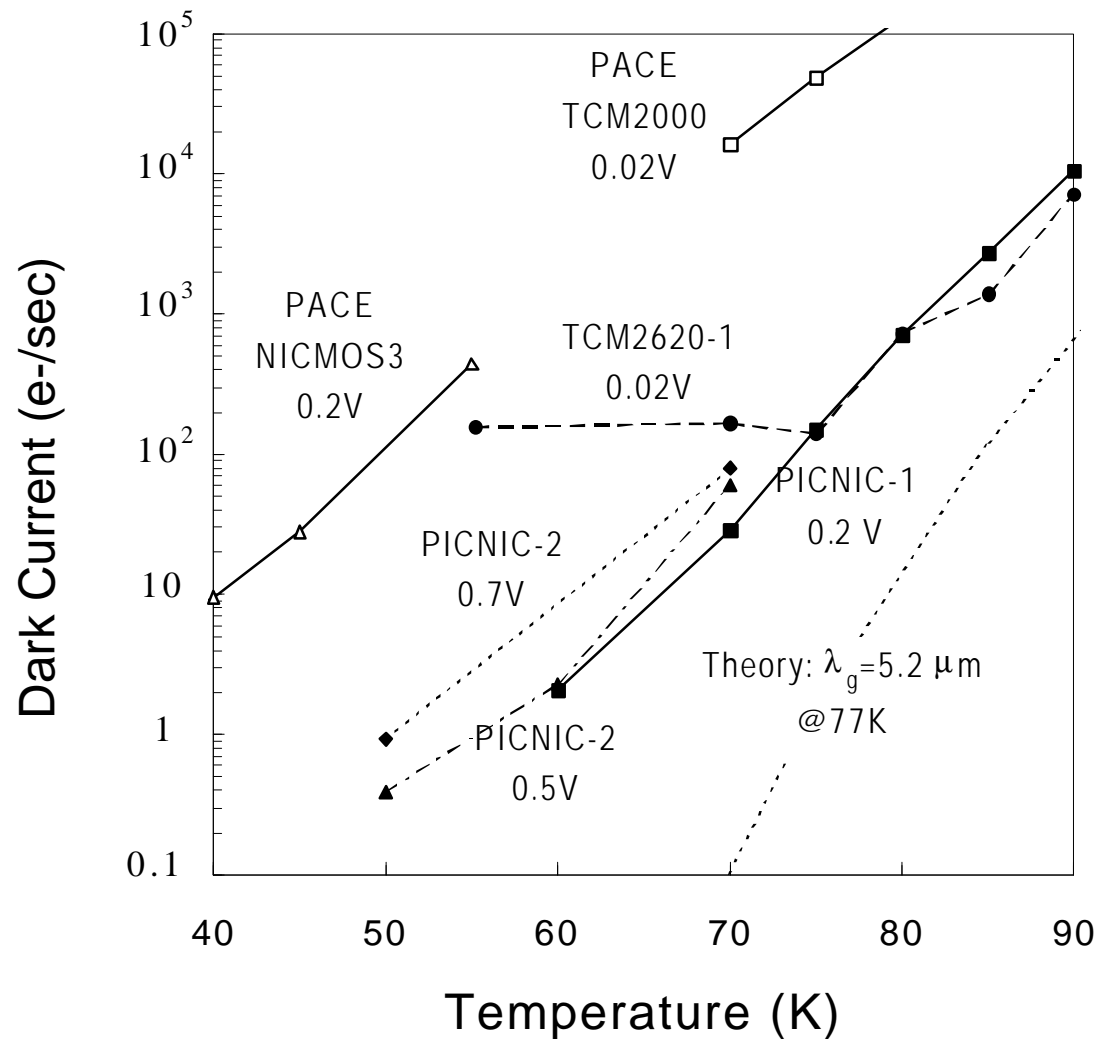
Thermally activated diffusion and G-R currents have strong T and λ_c dependence but weak bias dependence

Tunneling currents have strong bias and λ_c dependence but weak T dependence. Large pixel-to-pixel variations indicate that macro defects distributed randomly among pixels are the source.



FPA Median $I_{\text{dark}} = 0.39 \text{ e-/sec}$ at 50K for $\lambda_c = 5.2 \mu\text{m}$

RBB, NGST, 6/3/98, 9



PICNIC readout has SFD input. Dark current increases with detector reverse bias voltage.

TCM2620 readout circuit has CTIA input and operates near zero bias. Infrared self-emission of readout provides most of the measured current below 75K.

p-on-n DLPH detector arrays on CdZnTe substrates have 100x lower I_{dark} than n-on-p PACE detector arrays fabricated on sapphire substrates.

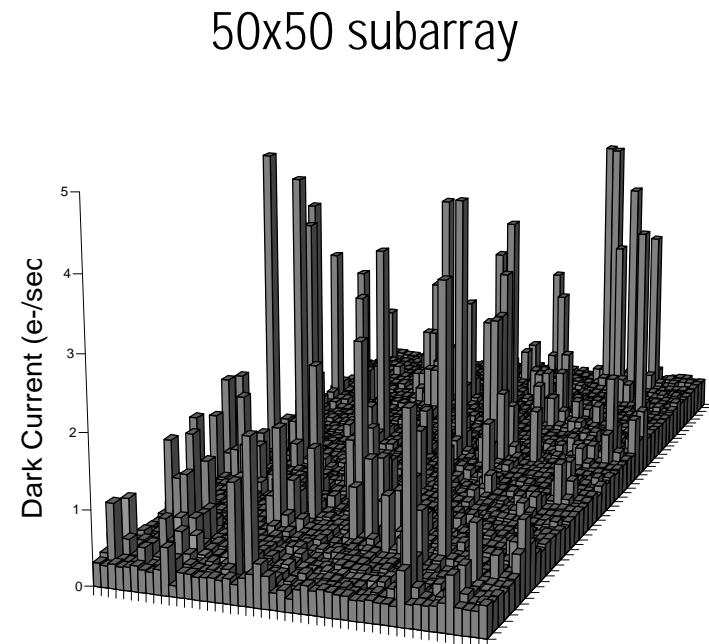
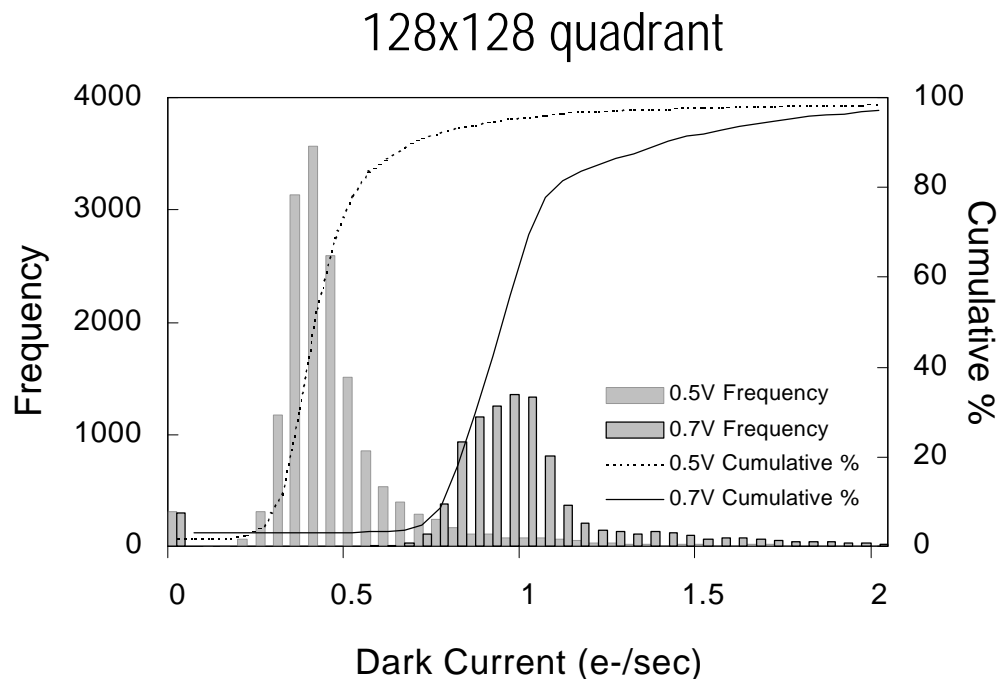
I_{dark} Distributions at 50K for FPA PICNIC-2 with $\lambda_c=5.2 \mu\text{m}$

RBB, NGST, 6/3/98, 10

Median I_{dark} increases from 0.39 e-/sec @ 0.5V bias to 0.95 e-/sec @ 0.7V.

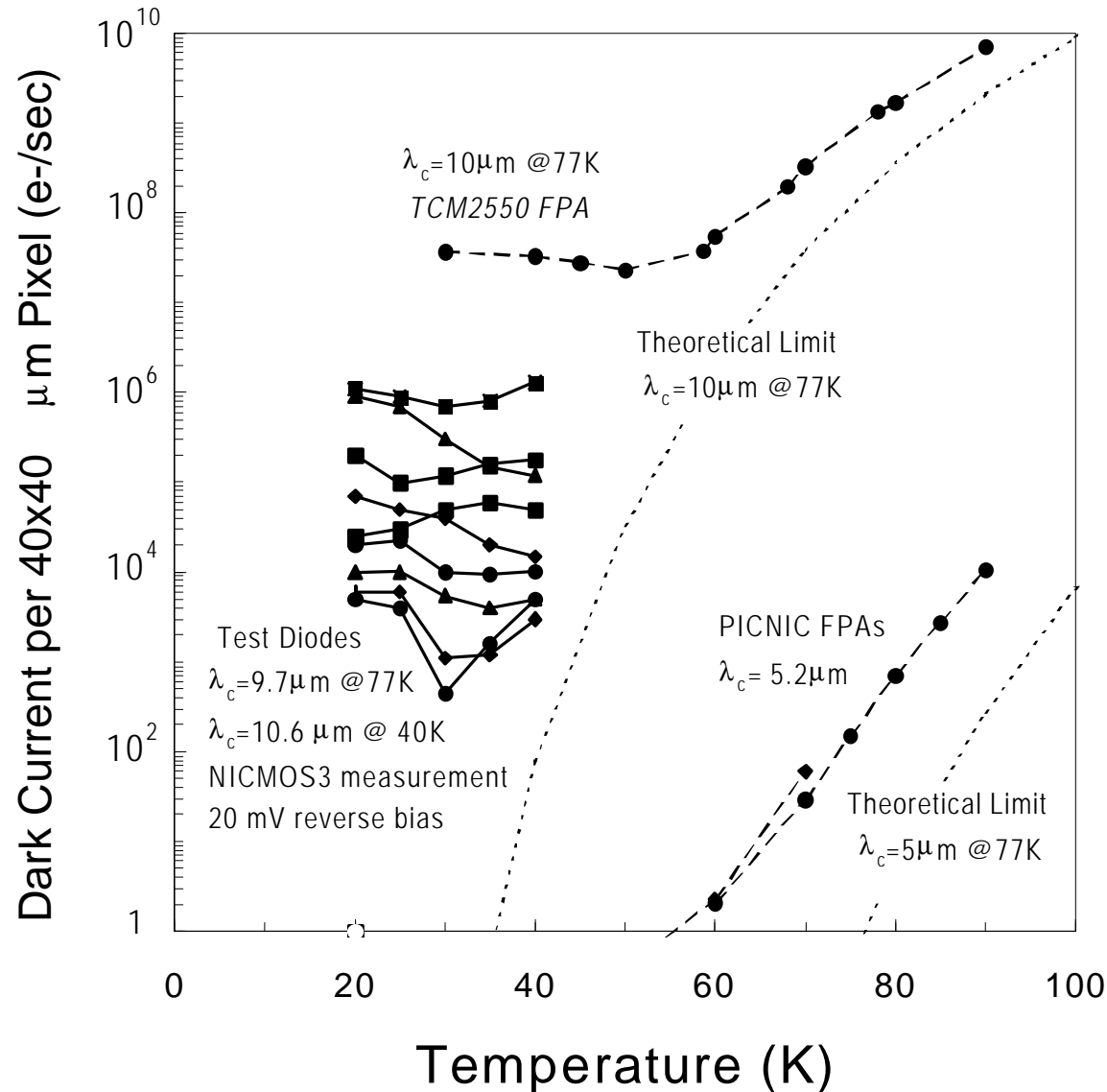
At 0.5V bias, 93.8% of pixels have $I_{\text{dark}} < 1\text{e-/sec}$.

High current pixels are distributed fairly randomly across array.



DLPH Test Detectors with $\lambda_c=10.6\mu\text{m}$ Show Promise

RBB, NGST, 6/3/98, 11

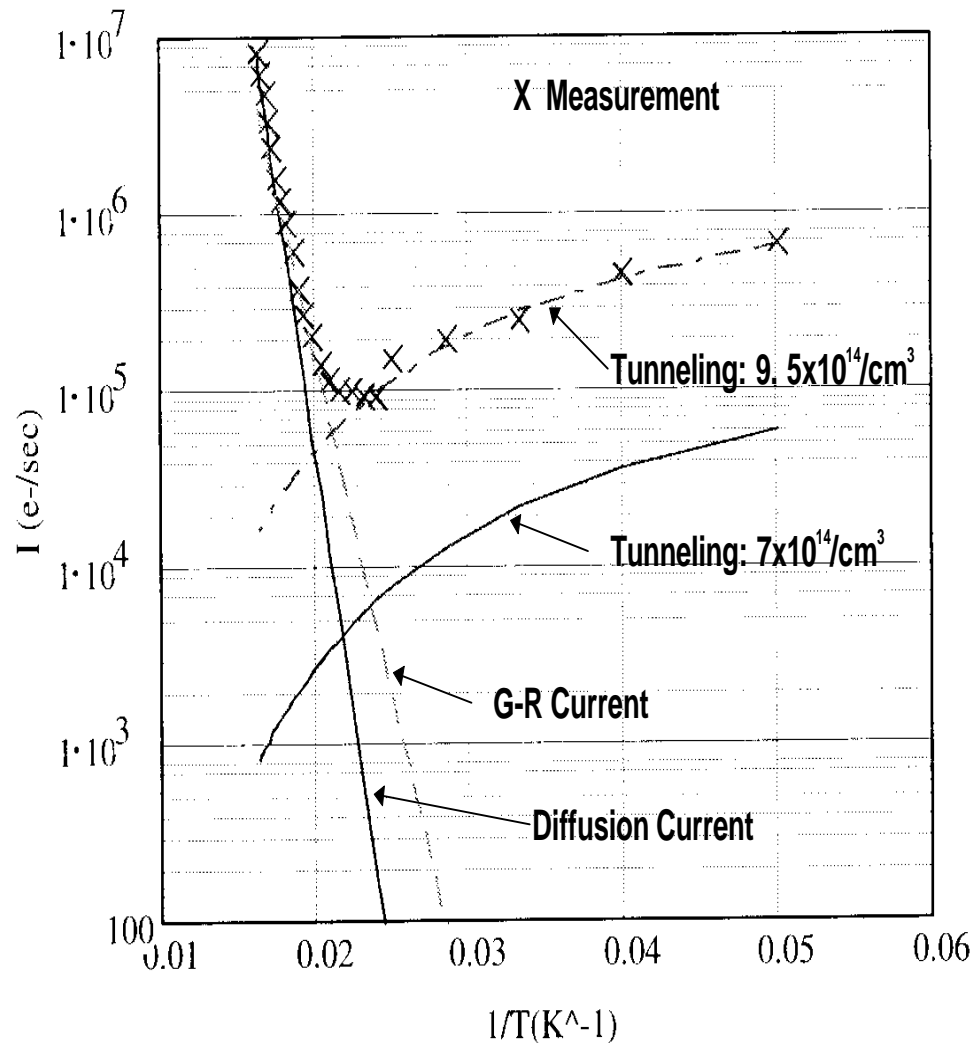


Typical 256x256 TCM2550 FPAs from baseline process have median dark currents $>2 \times 10^7$ e-/sec for $T=30\text{-}70\text{K}$.

Experimental test detectors, designed to minimize currents from crystal defects, have I_{dark} much closer to theoretical limits. They were wirebonded to NICMOS3 readout pixels for sensitive I-V measurements.

Tunneling Currents Decrease with DLPH Active Layer Donor Concentration N_d

RBB, NGST, 6/3/98, 12



$N_d = 9.5 \times 10^{14}$ for the $\lambda_c = 10.6$ μm test detectors

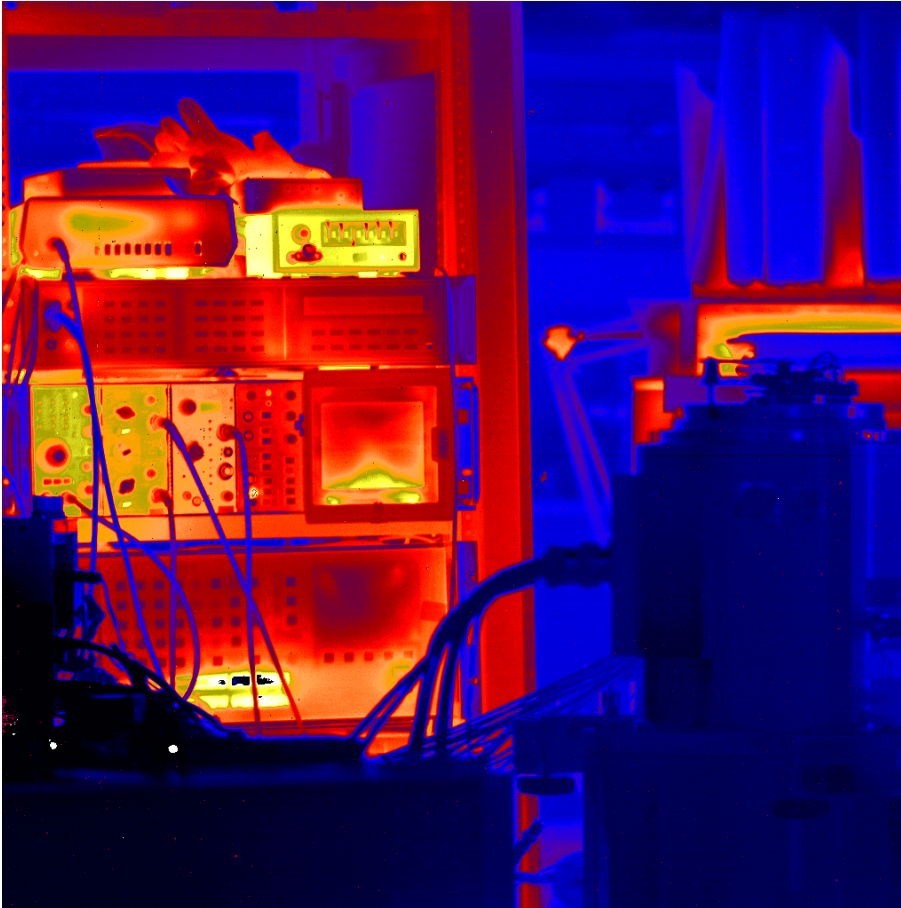
Current vs T measured at 100mV reverse bias was fit to model including diffusion, G-R, and tunneling current.

Model predicts 10x reduction in minimum dark current for $N_d = 7 \times 10^{14}$.

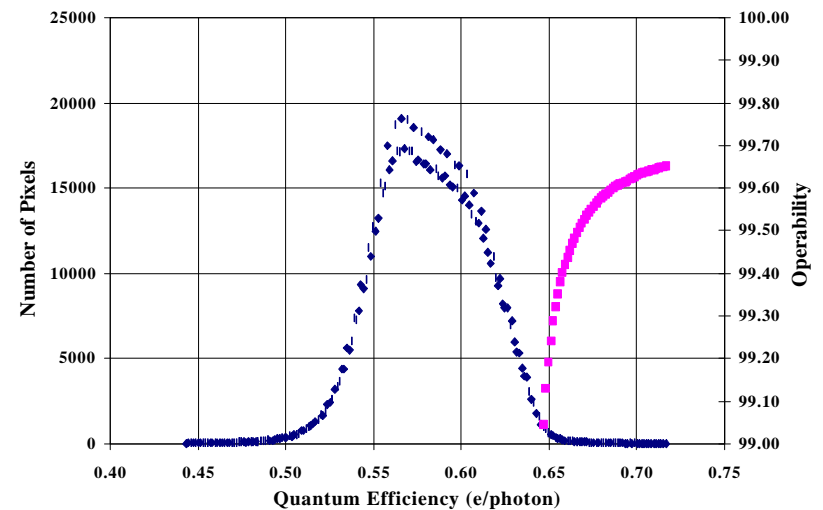
HgCdTe-on-Silicon 1024x1024 FPA Demonstrated

RBB, NGST, 6/3/98, 13

Laboratory Thermal Image, 77K, $f/2$, $\tau_{\text{int}} = 1$ ms



- MBE Detector layer 2-540, $\lambda_c = 4.2 \mu\text{m}$
- TCM8050 readout, $18 \mu\text{m}$ pitch
- Mean QE = 0.58
- Operability = 99.65% (pixels within 25% of mean QE)
- Std/Mean = 5.4%

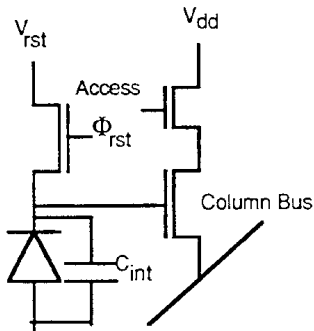


BOEING®

**Rockwell
Science Center**

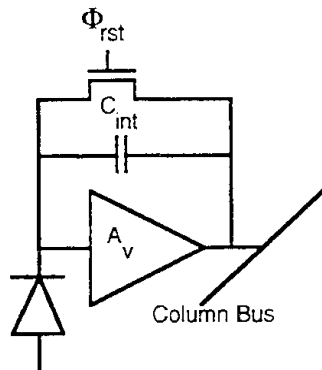
$\lambda_c \gg 5 \mu\text{m}$ Requires Different Mux Design

RBB, NGST, 6/3/98, 14



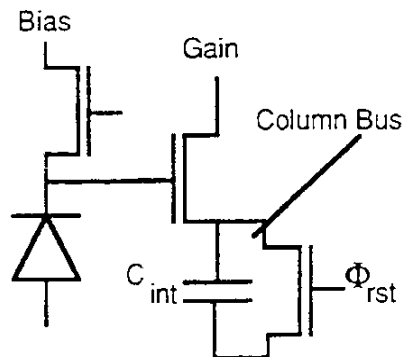
Source Follower per Detector (SFD) of NICMOS3 & HAWAII

- Signal integrates on reverse biased detector capacitance
- Dynamic range is limited by detector breakdown voltage
- Current flows in FETs only during reads not during integration



Capacitive Transimpedance Amplifier (CTIA)

- Mux feedback capacitor stores integrated detector current
- Amplifier maintains detector bias at nearly constant value that can be set close to zero.
- Infrared glow from FETs is proportional to amplifier current



Gate Modulation (GM)

- Can operate with high current gain to reduce read noise

Summary and Conclusions

RBB, NGST, 6/3/98, 15

- DLPH detectors and arrays fabricated on MBE grown HgCdTe crystal layers have demonstrated dark current performance useful for low background astronomical imaging at wavelengths between 5 and 10 μm .
- Operating temperatures for minimum dark current are above 30K so that passive cooling may be sufficient.
- More data is needed on detector arrays optimized for the NGST's very low background environment.